Orientational and Aggregational States of Magainin 2 in Phospholipid Bilayers†

Katsumi Matsuzaki,* Osamu Murase, Hideaki Tokuda, Susumu Funakoshi, Nobutaka Fujii, and Koichiro Miyajima

Faculty of Pharmaceutical Sciences, Kyoto University, Sakyo-ku, Kyoto 606-01, Japan

Received April 16, 1993; Revised Manuscript Received December 28, 1993®

ABSTRACT: Magainins from *Xenopus* skin are antimicrobial peptides with broad spectra, and their action mechanisms are considered to be the permeabilization of bacterial membranes. To elucidate their molecular mechanisms, three analog peptides of magainin 2, each having a Trp residue substituted for Phe at the 5th, 12th, or 16th position, were synthesized, and their interactions with acidic phospholipid membranes were investigated by fluorescence. The Trp substitution did not significantly affect the properties of the parent peptide. The binding isotherms of these peptides to the membranes, which were obtained on the basis of fluorescence changes upon membrane binding of the peptides, were sigmoidal, suggesting the association of the bound peptide molecules. A quantitative analysis indicated that the formed aggregate is a dimer. The observation that the initial rate constant of magainin 2 induced leakage of calcein from liposomes was dependent on the fourth power of the peptide concentration demonstrates the formation of a tetrameric pore. A blue shift and intensity enhancement of Trp fluorescence in the presence of the membranes indicate that those Trp residues are buried in the hydrophobic region of the bilayers. Furthermore, the depths of the Trp residues, which were determined using the *n*-doxylphosphatidylcholine quenching technique, were about 10 Å from the bilayer center irrespective of the peptide aggregational state. Thus, it was concluded that the orientation of the magainin 2 α-helix is parallel to the membrane surface. A model of the pore formation will be proposed on the basis of these observations.

Magainins 1 and 2, recently isolated from *Xenopus* skin, are antimicrobial peptides with broad spectra (Zasloff, 1987; Zasloff et al., 1988). Magainins consist of 23 amino acid residues and have net 4 positive charges: Gly-Ile-Gly-Lys-Phe^5-Leu-His-Ser-Ala-Gly^{10}(for magainin 1, Lys^{10} for 2)-Lys-Phe-Gly-Lys-Ala^{15}-Phe-Val-Gly-Glu-Ile^{20}-Met-Lys-(for 1, Asn for 2)-Ser. The channel-forming activity in planar bilayers (Cruciani et al., 1992; Duclohier et al., 1989), the disruption of the membrane potential of biomembranes (Westerhoff et al., 1989a,b), and the permeability enhancement of liposomes (Matsuzaki et al., 1989a, 1991a) indicate that the antimicrobial activity of magainins is primarily ascribable to their actions on bacterial membranes. Electrostatic interactions of magainins with acidic lipids are important in the membrane binding process (Matsuzaki et al., 1989a, 1991a), although at high concentrations magainin 2 amide solubilizes zwitterionic phosphatidylcholine membranes (Williams et al., 1990).

Knowledge of the orientational and aggregational states of the membrane-bound peptide molecules will give us a clue to clarify the detailed mechanisms of the activity for membranes. Magainins adopt mainly α-helical structures in trifluoroethanol/water mixtures as revealed by circular dichroism (CD)[1] (Chen et al., 1988) and NMR (Marion et al., 1988). Chen et al. (1988) also demonstrated that analog peptides with enhanced helix contents exhibit higher antimicrobial activities, suggesting the importance of helical structures. In phospholipid membranes, magainins also form helices (Matsuzaki et al., 1989a, 1991a; Williams et al., 1990) which are amphiphilic, as proposed by their primary sequences. Several lines of evidence suggest that the magainin helix lies parallel to the membrane surface. Thermal (Matsuzaki et al., 1991a) and Raman (Williams et al., 1990) studies demonstrated that the peptide-induced perturbation of lipid acyl chain conformations is minimal. Recently, Bechinger et al. (1991) showed, by measuring the ^{15}N amide chemical shift of ^{15}N-labeled Ala^{15} of magainin 2 (3 mol %) in phosphatidylglycerol/phosphatidylcholine bilayers, that the helix lies in the plane of the membrane. However, another approach would be helpful to confirm this conclusion, because (1) Ala^{15} may be near the end of the helix (Matsuzaki et al., 1991a; Williams et al., 1990), (2) the orientation may depend on the peptide content, and (3) the sample preparation method may affect the result. (They premixed the peptide and the lipids in an organic solvent.) As for the aggregational states of magainins, we have no information at present.

The fluorescence of a Trp residue is a useful source of molecular information about a membrane-bound peptide because of various available quenching techniques (Blatt & Sawyer, 1985; Bolen & Holloway, 1990; Chattopadhyay & London, 1987; Chung et al., 1992; De Kroon et al., 1990; Matsuzaki et al., 1991c; McKnight et al., 1991; Voges et al., 1987). Thus, we synthesized three analog peptides of magainin 2, each having a Trp residue substituted for a Phe residue at the 5th, 12th, or 16th position, and studied their interactions with egg yolk L-α-phosphatidyl-DL-glycerol (egg PG) liposomes to elucidate the orientation of the magainin helix in membranes. These Phe residues are at similar positions in the helical wheel representation (Figure 1). Furthermore, the spectral changes of Trp upon membrane binding enable us to estimate the binding isotherms of the peptide (Schwarz et al., 1987), which inform us of its intramembrane aggre-

† This work was supported in part by Grant-in Aid 02453144 for Scientific Research from the Ministry of Education, Science and Culture of Japan.

* To whom correspondence should be addressed. Telephone: 81-75-753-4574. Fax: 81-75-761-2698.

® Abstract published in *Advance ACS Abstracts,* February 15, 1994.

[1] Abbreviations: CD, circular dichroism; egg PC, egg yolk L-α-phosphatidylcholine; egg PG, L-α-phosphatidyl-DL-glycerol enzymatically converted from egg PC; *n*-doxyl-PC, 1-palmitoyl-2-stearoyl-(*n*-doxyl)-L-α-phosphatidylcholine; NBD-PE, *N*-(7-nitro-2,1,3-benzoxadiazol-4-yl)dipalmitoyl-L-α-phosphatidylethanolamine; LUVs, large unilamellar vesicles; SUVs, small unilamellar vesicles; MIC, minimal inhibitory concentration.

0006-2960/94/0433-3342$04.50/0

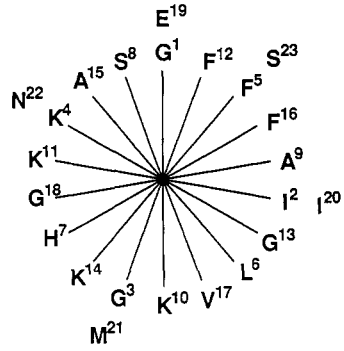

FIGURE 1: Helical wheel diagram of magainin 2.

gational state (Schwarz, 1989). Fluorescence quenching experiments by lipid quenchers will estimate the depth of each Trp residue in the membranes, from which we can discuss the orientation of the magainin helix. On the basis of membrane permeability data combined with these fluorescence results, we will propose a tentative model of the magainin pore.

MATERIALS AND METHODS

Materials. Magainin 2 and its three Trp-substituted analogs (5-, 12-, and 16-Trp magainin 2) were synthesized by a standard fluoren-9-ylmethoxycarbonyl (Fmoc)-based solid-phase method. The crude peptides were purified by HPLC (Matsuzaki et al., 1989a) and gel filtration (Sephadex G-15, 2.5 × 35 cm column, 0.02 N HCl being used as an eluent). The purities of the synthesized peptides were ascertained by quantitative amino acid analysis. Egg yolk L-α-phosphatidylcholine (egg PC) was a product of Sigma. L-α-Phosphatidyl-DL-glycerol enzymatically converted from egg PC (egg PG) was a gift of Nippon Fine Chemical Co. (Takasago, Japan). 1-Palmitoyl-2-stearoyl-(*n*-doxyl)-L-α-phosphatidylcholine [*n*-doxyl-PCs (*n* = 5, 10, and 12)] was purchased from Avanti Polar Lipids, and *N*-(7-nitro-2,1,3-benzoxadiazol-4-yl)dipalmitoyl-L-α-phosphatidylethanolamine (NBD-PE) was obtained from Molecular Probes. Calcein and spectrograde organic solvents were supplied by Dojindo (Kumamoto, Japan). All other chemicals from Wako (Tokyo, Japan) were of special grade. The spectroscopic measurements were carried out at 30 ± 0.5 °C in a Tris-HCl buffer (10 mM Tris/150 mM NaCl/1 mM EDTA, pH 7.0) prepared from water twice-distilled in a glass still.

Vesicle Preparation. Large unilamellar vesicles (LUVs) were prepared and characterized, as described elsewhere (Matsuzaki et al., 1991b,c). Briefly, a lipid film, after being dried under vacuum overnight, was hydrated with the Tris buffer or a 70 mM calcein solution (pH was adjusted to 7.0 with 1 N NaOH) and vortexed. The suspension was freeze-thawed for five cycles and then successively extruded through polycarbonate filters (a 0.6-μm pore size filter × 5 times, two stacked 0.1-μm pore size filters × 10 times). Calcein-entrapped vesicles were separated from free calcein on a Sephadex G-50 column. The lipid concentration was determined by phosphorus analysis (Bartlett, 1959). Small unilamellar vesicles (SUVs) for CD measurements were prepared from egg PG by sonication (Matsuzaki et al., 1991a).

CD Measurements. CD spectra of a 30 μM peptide/buffer solution in the absence or presence of 0.9 mM egg PG SUVs were recorded on a JASCO J-720 instrument interfaced to an NEC PC-9801 microcomputer, using a 1-mm path-length quartz cell to minimize the absorbance due to buffer components. The instrumental outputs were calibrated with nonhygroscopic ammonium *d*-camphor-10-sulfonate (Takakuwa et al., 1985). Eight scans were averaged for each sample. Averaged blank spectra (the vesicle suspension or the buffer) were subtracted. The reported spectra were the average of three independent preparations for each type of sample. The coefficients for variation were less than 7% at 222 nm. The absence of any optical artifacts was confirmed elsewhere (Matsuzaki et al., 1989b). The binding isotherms of the peptides to SUVs were obtained from changes in the mean residue ellipticity at 222 nm upon membrane binding, as previously described (Matsuzaki et al., 1991a). The isotherms were used to estimate the bound peptide fractions.

Fluorescence Measurements. Fluorescence measurements were carried out on a Shimadzu RF-5000 spectrofluorometer. In binding and quenching experiments, the Trp residue of the peptide was excited at 280 nm, and corrected emission spectra (Matsuzaki et al., 1991c) were recorded in the wavelength range 250–450 nm. Calcein fluorescence for leakage experiments was measured at an excitation wavelength of 490 nm and an emission wavelength of 520 nm.

Leakage Out of LUVs. Typically, small aliquots of calcein-entrapped vesicles were added to 2 mL of a peptide solution (0.5–2 μM) in a quartz cuvette, and the release of the dye was monitored by fluorescence. To investigate the detailed kinetics of leakage in the early stage, an RX-1000 stopped-flow apparatus (Applied Photophysics Ltd.) was used, and the leakage time course was recorded at 0.1-s intervals. The mixing dead time was less than 20 ms, according to the manufacturer. The maximum fluorescence intensity was determined by addition of 10% Triton X-100 (20 μL).

Binding Experiments. The binding of the three magainin analogs to LUVs composed of egg PG or egg PG/egg PC (4/1, mol/mol) was estimated on the basis of their Trp fluorescence. Peptide solutions, at least four different concentrations, were titrated with a vesicle suspension while the fluorescence spectra of the Trp residue were recorded after 10-min incubation for equilibration. Fluorescence data were averaged for three independent samples after volume correction for dilution (up to 3%). The standard deviations were less than 3%.

Quenching Experiments. LUVs for *n*-doxyl-PC quenching experiments were composed of egg PG/spin-labeled PC/egg PC (80/14/6). The concentration of actual spin-labeled lipid in each doxyl-PC was determined on the basis of the quenching of NBD-PE fluorescence (Chattopadhyay & London, 1987). Fluorescence intensities (336 nm) of the three analog peptides in the presence of these doxyl-containing vesicles were measured for three independent preparations and averaged. The standard deviations were less than 4%. The data were analyzed according to the parallax method by Chattopadhyay and London (1987). The distance between the bilayer center and the fluorophore, Z_{CF}, was calculated from eq 1 where C

$$Z_{CF} = -\frac{1}{2L_{m-n}}\left[\frac{1}{\pi C}\ln\left(\frac{F_m}{F_n}\right) + L_{m-n}^2\right] + L_{c-m} \quad (1)$$

is the two-dimensional concentration of the quenchers in the membranes (0.002 molecule/Å^2, assuming that the cross section of a lipid molecule is 70 Å^2). F_m and F_n are the fluorescence intensities in the presence of *m*- and *n*-doxyl-PC, respectively. L_{c-m} is the length between the bilayer center and the doxyl group of *m*-doxyl-PC [12.15, 7.65, and 5.85 Å for $m = 5$, 10, and 12, respectively (Chattopadhyay & London, 1987)]. The vertical length between the *m*- and *n*-doxyl groups, L_{m-n}, was obtained from these L_{c-m} values.

Antimicrobial Activities. Escherichia coli cells (ACTT 8739) were cultured in a minimum essential medium (g/L)

Table 1: Comparison between Magainin 2 and Trp-Substituted Analogs

peptide	$[\theta]_{222}$[a]	$[\theta]_{222}/[\theta]_{209}$	calcein leakage[b]	MIC[c]
magainin 2	-17.3×10^3	1.01	49.6	55.5
5-Trp magainin 2	-20.9×10^3	1.01	45.7	31.4
12-Trp magainin 2	-23.6×10^3	1.06	48.3	31.4
16-Trp magainin 2	-23.2×10^3	1.00	51.8	62.8

[a] Mean residue ellipticity of a peptide solution (30 μM) in the presence of 0.9 mM egg PG SUVs (in deg·cm²·dmol⁻¹). [b] Percent leakage of calcein out of egg PG LUVs for 1 min. Concentration: peptide, 1.5 μM; lipid, 203 μM. [c] Minimal inhibitory concentrations (in μM) against *E. coli*.

of 10 casein peptone/5 yeast extract/10 NaCl at 37 °C (Matsuzaki et al., 1991c). Then the cells were harvested in the midlogarithmic phase and resuspended in Hepes buffer. The peptides were sterilized through a filter (pore size, 0.22 μm) and stepwise-diluted. The bacterial cells were mixed with each peptide and the medium in a microplate well. The final composition of the bacterial suspension was 10 mM Hepes/150 mM NaCl/1% (w/v) casein peptone/0.5% (w/v) yeast extract/0–126 μM peptide/10^6 cfu/mL *E. coli* cells (pH 7.0). The bacterial growth was measured as the increase in optical density at 405 nm after incubation at 37 °C for 4 h.

RESULTS

Comparison between Analog Peptides and Parent Peptides. We synthesized the three Trp-substituted magainin 2 analogs to clarify the orientational and aggregational states of magainin 2 in membranes. Thus, it is of primary importance to confirm that these analogs do not differ significantly from the parent peptide in their membrane actions. We examined their antimicrobial activities against *E. coli*, membrane-permeabilizing abilities, and membrane-bound conformations (Table 1). The MIC values of these four peptides were in the range of 31.4–62.8 μM. Their dye-releasing activities were almost identical. Their CD spectra (data not shown), therefore conformations, were typical of a helix with double minima at 209 and 222 nm. The $[\theta]_{222}$ and $[\theta]_{222}/[\theta]_{209}$ values are listed in Table 1. The latter values may serve as diagnostics of interhelical interactions (Lau et al., 1984). Namely, coiled-coil structures will give the ellipticity ratios close to unity in contrast to 0.8 in monomeric helices.

Binding Isotherms. Binding isotherms inform us not only of the binding mode but also of the fraction of free peptide under a given experimental condition. The latter knowledge is essential for extracting information on the membrane-bound peptide from observed data. The binding isotherms of the three analog peptides were estimated on the basis of changes in fluorescence spectra upon binding to lipid vesicles. For example, Figure 2 shows the spectra of 5-Trp magainin 2 in the presence of various concentrations of egg PG LUVs. The binding of the peptide to the lipid membranes resulted in an intensity enhancement and a blue shift of the Trp fluorescence, implying that the Trp residue is located in the hydrophobic environment of the membrane. Figure 3 illustrates the fluorescence intensity enhancement at 336 nm as a function of the lipid concentration. At first, the intensities were monotonously increased with the lipid concentration. However, further addition of the vesicles slightly decreased the fluorescence of 5- and 12-Trp magainins, indicating that the quantum yields of the membrane-bound Trp residues are a function of the amount of the membrane-bound peptide per lipid molecule, r.

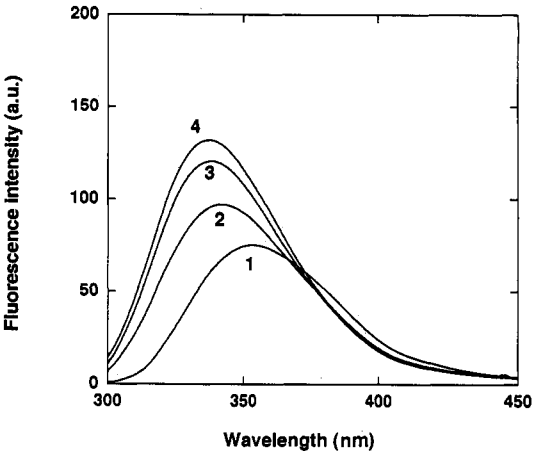

FIGURE 2: Fluorescence spectra of 5-Trp magainin 2 at 30 °C. A peptide solution (5 μM) was titrated with an egg PG vesicle suspension. The excitation wavelength is 280 nm. [L] (μM): curve 1, 0; curve 2, 17.0; curve 3, 31.0; curve 4, 109.

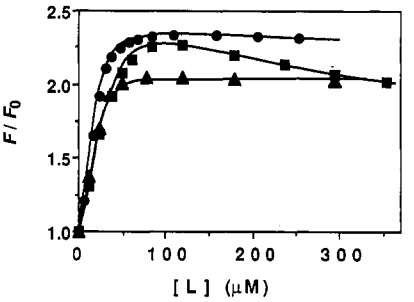

FIGURE 3: Fluorescence intensity enhancement of Trp-substituted magainins at 30 °C. F/F_0, the fluorescence intensity of a 5 μM peptide solution in the presence of lipid divided by that in the absence of lipid, was plotted as a function of lipid concentration, [L]. The excitation and emission wavelengths were 280 and 336 nm, respectively. Peptides: circles, 5-Trp magainin 2; squares, 12-Trp magainin 2; triangles, 16-Trp magainin 2.

However, there remains a possibility that the anomalous titration curves result from optical artifacts due to light scattering. Thus, we estimated the effects of vesicle-originated light scattering on the fluorescence spectra of indoxyl sulfate (excited at 280 nm), which is expected to have no interactions with egg PG vesicles because of electrostatic repulsions. The presence of 1 mM LUVs, which showed an OD value as high as 0.43 at the excitation wavelength, *never* affected the fluorescence spectra after subtraction of the corresponding blank spectra (data not shown).

The fluorescence intensity of the peptide solution in the absence (F_0) and presence (F) of lipid vesicles is expressed by eq 2, where $[P]_0$, $[P]_b$, and $[P]_f$ are the total, bound, and free peptide concentrations, respectively.

$$F_0 = k_f[P]_0 \tag{2a}$$

$$F = k_f[P]_f + k_b[P]_b = k_f[P]_f + k_b r[L] \tag{2b}$$

Here k represents a coefficient proportional to the quantum yield and the subscripts f and b refer to the free and bound states of the peptide, respectively. [L] denotes the lipid concentration. For the three peptides, the coefficient k_f values were constant in the experimented concentration range (0.5–5 μM). These results guarantee negligible adsorption of the peptides to cuvettes or pipet chips. However, k_b is considered to be a function of r, as mentioned above. From eq 2, eq 3 is obtained.

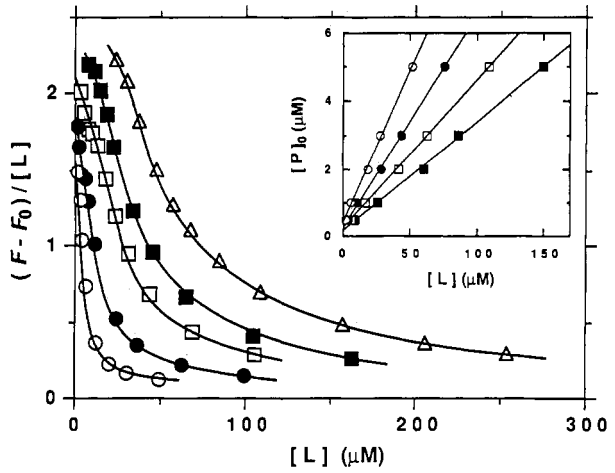

FIGURE 4: Estimation of the binding isotherm in the 5-Trp magainin 2–egg PG system. $(F-F_0)/[L]$ versus [L] plots at various $[P]_0$. $[P]_0$ (μM): open circles, 0.5; closed circles, 1; open squares, 2; closed squares, 3; open triangles, 5. Inset: Linear relations between [L] and $[P]_0$ plotted according to eq 4. $(F-F_0)/[L]$ values: open circles, 1.4; closed circles, 1.0; open squares, 0.7; closed squares, 0.5.

$$(F - F_0)/[L] = (k_b - k_f)r \quad (3)$$

Thus, $(F - F_0)/[L]$ is a function of only r via k_b. Figure 4 shows plots of $(F - F_0)/[L]$ vs [L] at various total peptide concentrations, $[P]_0$. Five points exhibiting a given $(F-F_0)/[L]$ value (e.g., unity) at different $[P]_0$ values should have the same r value and the corresponding $[P]_f$ value. The r and $[P]_f$ values for this $(F - F_0)/[L]$ value can be estimated by the material balance equation:

$$[P]_0 = [P]_f + r[L] \quad (4)$$

because the r and $[P]_f$ values are constant for these five points. The r and $[P]_f$ values were obtained from the slopes and the intercepts, respectively, of the linear relations (eq 4) in the inset of Figure 4.

Figure 5 shows the relation between r and $[P]_f$ (binding isotherms). The similar isotherms of the three analogs were sigmoidal in both membrane systems.

Fluorescence Quenching. To precisely estimate the depths of the Trp residues in the bilayer, we carried out fluorescence quenching experiments using *n*-doxyl-PCs (n = 5, 10, and 12). According to the parallax method (Chattopadhyay & London, 1987), Z_{CF} values, the transversal distances between the bilayer center and the Trp residues, were calculated from eq 1. For each peptide, a triplet of Z_{CF} values obtained from the combination of the three doxyl-PCs was averaged. The standard deviations were about 0.6 Å. In Figure 6, the Z_{CF} values for 5-, 12-, and 16-Trp magainin 2 were plotted as a function of r. The vertical axis scale (15 Å) corresponds to the thickness of the hydrophobic region of one leaflet of the bilayer. The Z_{CF} values were 8–10 Å for all the analog peptide Trp residues irrespective of r. Transleaflet quenching did not occur according to the criteria by Chattopadhyay and London (1987).

Leakage. As a measure of membrane permeabilization, we examined the leakage of calcein from egg PG vesicles. Two modes can be considered in the dye release, i.e., the "graded" mode and the "all-or-none" mode (Parente et al., 1990). In the former mode, all the vesicles release some of their contents. The leakage occurs through this process if the lifetime of the pore is not long enough to deplete the intravesicular contents. This lifetime is estimated to be ca. 15 ms in our case (pore area = 0.3 nm², vesicle radius = 50 nm) according to Schwarz and Robert (1992). In contrast, in the latter case, some vesicles leak all of their contents, whereas the other vesicles remain intact. Information on the leakage mode is also necessary to calculate the percent leakage value (Weinstein et al., 1981). These two modes are distinguishable by determination of the intravesicular dye concentration after peptide treatments (Weinstein et al., 1984). The percent self-quenching of calcein after peptide treatments was measured. After incubation with the peptides for 13 min, the vesicle fraction was separated from leaked calcein by gel filtration (Sephadex G-50), and the percent self-quenching value was obtained by measuring the fluorescence intensity before and after addition of Triton X-100. The dependency of the percent self-quenching value on the intravesicular calcein concentration has been published elsewhere (Matsuzaki et al., 1993a). If the leakage is the "all-or-none" event, the percent quenching value will be equal to the value before mixing with the peptides (0.89) whereas in the case of the "graded" leakage a lower self-quenching value will be observed because of the dilution of the intravesicular calcein solution. In the latter case, the percent leakage value, which is nonlinear relative to the measured fluorescence intensity, was obtained graphically from a calibration curve converted from the self-quenching curve of calcein (Matsuzaki et al., 1993a) according to Weinstein et al. (1981). Table 2 summarizes the percent self-quenching values after peptide treatments followed by separation from leaked free calcein, indicating that the dye leaks in the graded mode. Thus, we can conclude that the average lifetimes of a "pore" formed by the magainin peptides are less than ca. 15 ms² and that there exist instants in which no pore is open in each vesicle.

The time course of the flow of a marker from vesicles can be expressed by first-order kinetics on the basis of Fick's first

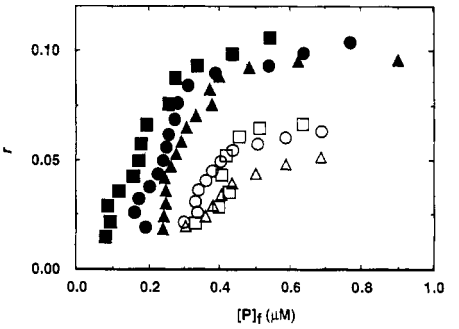

FIGURE 5: Binding isotherms of 5-, 12-, and 16-Trp magainins to egg PG containing LUVs at 30 °C. Peptides: circles, 5-Trp magainin 2; squares, 12-Trp magainin 2; triangles, 16-Trp magainin 2. Lipids: open symbols, eggPG/eggPC = 8/2; closed symbols, egg PG only.

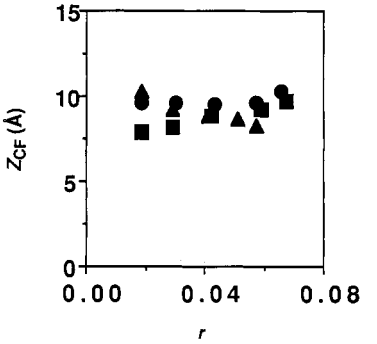

FIGURE 6: Location of Trp residues of 5-, 12- and 16-Trp magainins in phospholipid membranes. Z_{CF}, the distance between the Trp residue of each peptide and the bilayer center, was calculated from eq 1 and plotted as a function of r, bound peptides per lipid. Symbols are the same as in Figure 3.

Table 2: Modes of Magainin-Induced Calcein Leakage

peptides	observed[a]	predicted graded[b]	predicted all-or-none
magainin 2	69.8 ± 1.0	72.3	89.2
5-Trp magainin 2	72.5 ± 0.6	73.0	89.2
12-Trp magainin 2	70.3 ± 1.9	67.8	89.2
16-Trp magainin 2	69.4 ± 0.2	65.5	89.2

[a] Percent self-quenching values of intravesicular calcein after 13-min incubation with each peptide. Average of three independent samples ± standard deviation. [b] Calculated according to Weinstein et al. (1981).

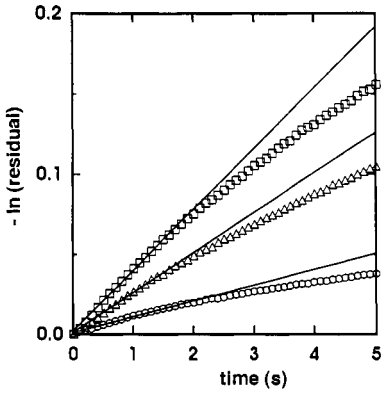

FIGURE 7: Initial kinetics of magainin 2-induced leakage of calcein from egg PG LUVs at 30 °C. –ln(residual) values were plotted as a function of time. The lines are obtained by linear regression. The lipid concentration was 129 μM. Peptide concentration (μM): circles, 0.8; triangles, 1.0; squares, 1.1.

law (Schwarz & Robert, 1992) (eq 5). [The extravesicular

$$\ln(\text{residual}) = -kt \quad (5)$$

dye concentration (μM) is negligible compared to the intravesicular one (mM).] Here, k is a leak rate coefficient which is related to the mean pore lifetime and the pore density. Figure 7 shows –ln(residual) vs t plots. The curves were not linear with decreasing slopes, indicating the presence of a pore deactivation process. Figure 8 depicts that the initial rate constant, k_0, was dependent on the fourth power of the peptide to lipid ratio, which is almost equal to the r values under these experimental conditions (Figure 5). These results suggest the involvement of peptide aggregation in dye leakage.

DISCUSSION

Elucidation of the conformational, orientational, and aggregational states of magainin in lipid membranes is crucial to reveal the molecular mechanisms of its antimicrobial activity, because its bactericidal action has been considered to involve the permeabilization of bacterial cell membranes (Cruciani et al., 1992; Duclohier et al., 1989; Matsuzaki et al., 1989a, 1991a; Westerhoff et al., 1989a,b; Zasloff, 1987; Zasloff et al., 1988). As for the peptide conformation, CD (Matsuzaki et al., 1989a, 1991a) and vibrational (Jackson et al., 1992; Williams et al., 1990) spectroscopic studies demonstrate that the conformations of membrane-bound magainins are mainly helical with some nonhelical structures, the latter being adopted by C-terminal negatively charged portions (Matsuzaki et al., 1991a, 1993b). Regarding the orientation

[2] Grant et al. (1992) reported that magainin 2 amide leaks a fluorescent dye, 6-carboxyfluorescein, from phosphatidylserine SUVs in the all-or-none mode. We also found that magainin 2 induced the all-or-none release of calcein from egg PG SUVs (unpublished work). Thus, the pore lifetime is longer than about 1 ms (Schwarz & Robert, 1992).

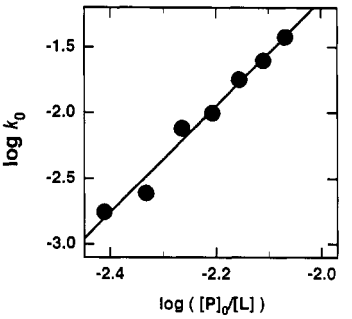

FIGURE 8: Dependence of the initial leakage rate constant, k_0, on the peptide/lipid ratio, $[P]_0/[L]$. The k_0 values were obtained from Figure 7. The slope of the regression line is 4.04.

and aggregation, few data are available. Thus, we synthesized the three Trp-substituted variants to shed light on these points using the fluorescence properties of Trp. We have taken the strategy of preparing 5-, 12-, and 16-Trp magainins for the following reasons. First, these residues are located at similar positions in the helical wheel representation (Figure 1). This is important in simplifying the interpretation of quenching data (Chung et al., 1992). Second, substitution between Trp and Phe is known not to affect the antimicrobial activity of cecropin (Steiner et al., 1988). As expected, our magainin 2 analogs have properties very similar to those of the underivatized peptide (Table 1).

Aggregation. The binding isotherms (Figure 5), CD spectra (Table 1), and leakage kinetics (Figure 8) argue for the involvement of peptide aggregation in pore formation. First, binding isotherms are known to reflect intramembrane peptide–peptide interactions (Schwarz, 1989). Estimation of binding isotherms requires discrimination between the bound and free peptides, which has been carried out using fluorescence (this work; Rizzo et al., 1987; Schwarz et al., 1987), CD (Beschiaschvili & Seelig, 1990a; Matsuzaki et al., 1991a; Rizzo et al., 1987; Schwarz & Beschiaschvili, 1989), and membrane permeabilization (Matsuzaki et al., 1989a,b, 1991a,c). Although these methods are indirect, they are established to give reasonable estimates, because isotherms obtained by two different methods are identical (Matsuzaki et al., 1991a; Rizzo et al., 1987). In fact, we have confirmed by use of SUVs that the binding isotherm of 16-Trp magainin 2 evaluated from CD titration was superimposable on that from fluorescence titration (data not shown). The detailed theoretical backgrounds for the indirect methods have been described by Schwarz et al. (1987). The same concept has been applied to studies of hemolysis (Matsuzaki et al., 1988; Thron, 1964) and protein–ligand interactions (Halfman & Nishida, 1972).

We have determined the binding isotherms on the basis of fluorescence changes while titrating peptide solutions with LUV suspensions. The implicit assumptions are fast redistribution of peptide molecules between the vesicles upon titration and the absence of r value-dependent morphological changes of the vesicles. The former seems to be valid, because we observed that dye leakage ceased immediately after addition of dye-free vesicles (data not shown). As for the latter assumption, we monitored 90° light-scattering intensity at 400 nm as a measure of vesicular aggregation during the titration experiment. At higher peptide to lipid ratios, we noticed only a small extent of vesicular aggregation, which was found to be reversible. Thus, we can safely interpret the obtained isotherms.

The sigmoidal isotherms of the magainin analogs (Figure 5) can be qualitatively explained as follows (Schwarz, 1989). If the membrane-bound peptide molecules are independent of

each other, the isotherm is expected to be linear through the origin (partition equilibrium). The observed upper bending of the isotherms in the r range of 0.02–0.07 (0.02–0.04) for pure egg PG (egg PG/egg PC mixture) strongly indicates intramembrane peptide aggregation. Accumulation of the positively charged peptide molecules reduces the surface negative charge of the membranes, weakening electrostatic interactions between the peptides and the lipids. This effect will cause a downward curvature, which was observed at higher r value.

Earlier quantitative studies on the binding of charged peptides to membranes were based on a mass-action equation with a defined number of lipids constituting a peptide "binding site" (Batenburg et al., 1987; Dufourcq & Faucon, 1977; Stankowski, 1983). Pseudocooperativity was deduced in some cases (Klotz, 1946; Stankowski, 1983). However, recent studies have demonstrated that such a Scatchard analysis, while empirically satisfying, provides a physically unrealistic picture of peptide binding and that the binding isotherm should be analyzed on the basis of partition equilibrium combined with the Gouy–Chapman theory, which takes electrostatic interactions into account (Beschiaschvili & Seelig, 1990a,b; Schwarz & Beschiaschvili, 1989). Unfortunately, this theory does not work in membranes containing high contents of phosphatidylglycerol (Macdonald & Seelig, 1987). Nevertheless, we can evaluate the molecularity, n, of the magainin aggregate by analysis of the steepest part (r = 0.04–0.07) of the isotherms for pure egg PG membranes (Figure 5), where we can assume that most peptide molecules are in the aggregated form. Thus, we can write

$$r \approx n r_n = n K_n K^n [P]_f^n \quad (6)$$

Here, r_n represents the number of n-mer per lipid; K_n and K ($=r_1/[P]_f$) denote an aggregation coefficient and a buffer–membrane partition coefficient, respectively. The parameter K is generally a function of r, because the r value determines the membrane surface charge density. However, we can approximate that K is constant in this narrow range of r: We have recently found (K. Matsuzaki and J. Seelig, unpublished work) that the effective charge of 16-Trp magainin 2 is about 2. Thus, a change in r from 0.04 to 0.07 leads to the maximum change in the extent of neutralization of the membrane negative charge from 16 to 28%, assuming that the peptide is localized on the outer leaflet. This extent of change does not significantly affect the membrane surface potential (Winiski et al., 1986). The n (R^2) values estimated from the slopes of the log r – log $[P]_f$ plots (data not shown) were 2.6 ± 0.3 (0.99), 2.3 ± 0.2 (0.97), and 1.9 ± 0.1 (1.00) for 5-, 12-, and 16-Trp magainin 2, respectively. In the case of egg PG/egg PC (80/20), a similar analysis (r = 0.03–0.04) led to n (R^2) values of 2.2 ± 0.3 (0.95), 2.8 ± 1.2 (0.66), and 1.8 ± 0.3 (0.95), respectively. Thus, the aggregate appears to be a dimer or a trimer. The latter is unconceivable because of larger scattering of the data leading to larger n values (also vide infra).

Second, the CD data (Table 1) supported the association of the peptide molecules bound to the membranes. The $[\theta]_{222}/[\theta]_{209}$ values close to unity are indicative of interhelical interactions, i.e., a coiled-coil structure (Lau et al., 1984). In contrast, this ratio of monomeric magainin 2 (30 μM in a 20 mM SDS solution, one peptide molecule per micelles) was 0.93. The possibility of aromatic side chain contributions to the observed CD spectra should be taken into account. However, as far as the parent peptide is concerned, such contributions are negligible (Dr. H. Kodama, personal communication).

Finally, the initial leakage rate coefficient, k_0, depended on the fourth power of the peptide to lipid ratio (Figure 8), indicating that peptide aggregation involves pore formation. Here we discuss pore formation kinetics. Figure 7 indicates that leakage occurs without any detectable delay and that the rate coefficient k, thus the number of pores, gradually decreases. The presence of pore deactivation processes has been reported for alamethicin (Schwarz & Robert, 1990), melittin (Schwarz et al., 1992), and magainins (Grant et al., 1992), although their natures have not been revealed. We confine ourselves to the very initial process where no deactivation occurs. In the linear portion of Figure 7, the number of pores (slope) is constant with respect to time, indicating the pores are formed immediately (≤1 s) after addition of the vesicles to the peptide solution. The partition of peptides to membranes is known to be accomplished in a millisecond order (Schwarz & Beschiaschivili, 1989; Schwarz et al., 1987). Thus, we can express the process as

$$m r_1 \overset{\text{fast}}{\rightleftarrows} r_m \rightarrow \text{leakage} \quad (7)$$

$$k_0 \propto r_m = K_m r_1^m \quad (8)$$

The meanings of the symbols are similar to those of eq 6. The leakage occurs at very low $[P]_0/[L]$ values (0.002–0.01, see Table 1) where most peptide molecules are in the bound state and significant aggregation does not occur (Figure 5). Therefore, we can approximate that $r_1 \approx [P]_0/[L]$. Figure 8 and eq 8 suggest that a magainin pore is formed by four monomers.

Orientation. We have hypothesized a model (Matsuzaki et al., 1991a) in which the magainin amphiphilic helix lies parallel to the membrane surface with its hydrophobic surface slightly embedded in the acyl chain region of the membrane. In this study, we have succeeded in confirming this model. Minimal perturbation of the lipid order (Matsuzaki et al., 1991a; Williams et al., 1990) supports this picture. Recently, Opella's group has reported the parallel orientation of ^{15}N-Ala^{15}-magainin 2 at a peptide to lipid ratio of 0.03 (Bechinger et al., 1991). The orientation might depend on the r value. Accordingly, we have estimated the orientation of magainin 2 as a function of r using the parallax method (Chattopadhyay & London, 1987) which can predict the depth of a chromophore in membranes within a couple of angstroms. Figure 6 indicates that all Trp residues are buried at 8–10 Å from the bilayer center in the range of r = 0.02–0.07, where intramembrane peptide aggregation occurs (Figure 5). These results strongly suggest the parallel orientation of the helix, because the transbilayer orientation would locate the Trp^5, Trp^{12}, and Trp^{16} residues at ca. 10, 0, and 6 Å from the bilayer center, respectively.[3] Such an orientation is a reasonable one as judged from the amphiphilicity of magainin. Inspection of Figure 1 reveals that the "hydrophobic angle" is almost equal to the "hydrophilic angle", suggesting the surface-seeking property of the peptide (Brasseur, 1991).

Pore Model. The positively charged N-terminal portion (from the N-terminus to at least Lys^{14}) of magainin binds to lipids to form an amphiphilic helix (Matsuzaki et al., 1991a, 1993b). Cuervo et al. (1988) reported that the first 12 residues must be intact for antimicrobial activity. The helix lies parallel

[3] This method can measure only the distance of a chromophore from the bilayer center. Thus, it can neither predict the localization of the peptides on the outer membrane leaflet nor determine if the membrane-spanning helices are parallel or antiparallel. A vesicle with quenchers in the outer membrane leaflet only would distinguish these possibilities.

to the membrane surface in such a way that the hydrophobic surface of the helix slightly penetrates the hydrophobic region of the membrane (Figure 6). The helix forms a dimer at r values higher than ca. 0.03 (Figure 5). If the whole length of the peptide molecule forms an amphiphilic helix, +8 charged dimer, ca. 35 Å in length, can bind a total of 8 acidic phospholipid molecules of 8–9 Å in diameter on both its sides. Thus, the dimer formation is electrically and dimensionally reasonable. Cruciani et al. (1992) proposed that magainin forms an antiparallel dimer, which can be stabilized through (1) dipole–dipole interactions and salt bridges between adjacent helices, (2) aromatic–aromatic interactions of the Phe^5 side chain of one helix with the Phe^{12} or Phe^{16} side chain of the adjacent helix, and (3) very tight side chain packing between adjacent helices. Our results are compatible with this model. First, our preliminary study (Matsuzaki et al., 1993b) has shown that deletion of the C-terminal negative charges (Glu^{19} and terminal COOH), which makes the peptide incapable of forming salt bridges, significantly reduces membrane permeabilization. Second, the presence of maxima in the fluorescence titration curves (Figure 3) may reflect the aromatic–aromatic interactions upon dimer formation.

In the r range of 0.002–0.01, the LUVs leak calcein (Table 1), K^+, and I^- ions (K. Matsuzaki et al., unpublished work). The binding isotherms (Figure 5) predict that the peptide molecules do not significantly aggregate under these leakage-occurring conditions, indicating that an aggregated minor population of membrane-bound peptides constitutes the short-lived pore. (A pore per vesicle is sufficient to cause the leakage.) The pore is constituted by a tetramer (Figure 8). The molecularity of 4 is in keeping with other studies. Westerhoff et al. (1989a) have reported that the respiration rate in rat liver mitochondria depends on the fourth power of the magainin concentration. Furthermore, we analyzed the ion channel data by Duclohier et al. (1989) and estimated that the number of peptide molecules involved in the ion channel is 4–6. The pore may be a transmembrane channel-like structure. If the pore were stable, the binding isotherm at high r values should be characteristic of tetramer formation, and the orientation (Figure 6) should change with the r value. Taking into consideration the presence of the pore-deactivating process (Figure 7; Grant et al., 1992) and the short life span of the pore (Table 2), we can conclude that the pore is a transient structure.

We hypothesize a tentative pore model. Accumulation of the peptide (monomer and dimer) exclusively in the outer leaflet of the bilayer leads to an unfavorable expansion of the monolayer. As a relaxation process, some peptide molecules are transferred to the inner leaflet through a transient porelike tetramer. Tetramer formation can translocate the peptide without exposing the hydrophilic residues to the hydrophobic interior of the bilayer. Import of a mitochondrial presequence peptide into phospholipid vesicles has been recently reported (Maduke & Roise, 1993). The tetramer pore seems to be too small to allow the dye molecule to pass. However, if a peptide–lipid complex constitutes the pore (Cruciani et al., 1992), the pore diameter will become larger, or the dye may move through a transient perturbation of membrane structure upon peptide translocation. The peptide molecules transferred to the inner leaflet are again in the monomer–dimer equilibrium, which is predicted by the isotherms (Figure 5). It should be noted that the binding isotherm gives us information of the system in the *equilibrium* state after the pore inactivation process, whereas the kinetic study indicates the *dynamics* of the initial stage. Thus, the peptide molecule exists as the dimer, which lies parallel to the membrane surface, even at higher r values after transient transmembrane tetramer formation during the translocation. In the case of other amphiphilic peptides, the same mechanism could explain pore formation. Melittin (Schwarz et al., 1992) and tachyplesin (Matsuzaki et al., 1991c) are known to form pores in membranes with the inactivation process. They orient essentially parallel to the membrane surface (Frey & Tamm, 1991; Matsuzaki et al., 1993c). The detailed pore formation mechanisms remain a subject of further study.

ACKNOWLEDGMENT

We thank Nippon Fine Chemical Co. for their kind gift of egg PG.

REFERENCES

Bartlett, G. R. (1959) *J. Biol. Chem. 234*, 466–468.
Batenburg, A. M., Hibbeln, J. C. L., & De Kruijff, B. (1987) *Biochim. Biophys. Acta 903*, 155–165.
Bechinger, B., Kim, Y., Chirlian, L. E., Gesell, J., Neumann, J.-M., Montal, M., Tomich, J., Zasloff, M., & Opella, S. J. (1991) *J. Biomol. NMR 1*, 167–173.
Beschiaschvili, G., & Seelig, J. (1990a) *Biochemistry 29*, 52–58.
Beschiaschvili, G., & Seelig, J. (1990b) *Biochemistry 29*, 10995–11000.
Blatt, E., & Sawyer, W. H. (1985) *Biochim. Biophys. Acta 822*, 43–62.
Bolen, E. J., & Holloway, P. W. (1990) *Biochemistry 29*, 9638–9643.
Brasseur, R. (1991) *J. Biol. Chem. 266*, 16120–16127.
Chattopadhyay, A., & London, E. (1987) *Biochemistry 26*, 39–45.
Chen, H.-C., Brown, J. H., Morell, J. L., & Huang, C. M. (1988) *FEBS Lett. 236*, 462–466.
Chung, L. A., Lear, J. D., & DeGrado, W. F. (1992) *Biochemistry 31*, 6608–6616.
Cruciani, R. A., Barker, J. L., Durell, S. R., Raghunathan, G., Guy, H. R., Zasloff, M., & Stanley, E. F. (1992) *Eur. J. Pharmacol. 226*, 287–296.
Cuervo, J. H., Rodriguez, B., & Houghten, R. A. (1988) *Pept. Res. 1*, 81–86.
De Kroon, A. I. P. M., Soekarjo, M. W., De Gier, J., & De Kruijff, B. (1990) *Biochemistry 29*, 8229–8240.
Duclohier, H., Molle, G., & Spach, G. (1989) *Biophys. J. 56*, 1017–1021.
Dufourcq, J., & Faucon, J.-F. (1977) *Biochim. Biophys. Acta 467*, 1–11.
Frey, S., & Tamm, L. K. (1991) *Biophys. J. 60*, 922–930.
Grant, E., Jr., Beeler, T. J., Taylor, K. M. P., Gable, K., & Roseman, M. A. (1992) *Biochemistry 31*, 9912–9918.
Halfman, C. J., & Nishida, T. (1972) *Biochemistry 11*, 3493–3498.
Jackson, M., Mantsch, H. H., & Spencer, J. H. (1992) *Biochemistry 31*, 7289–7293.
Klotz, I. M. (1946) *Arch. Biochem. Biophys. 9*, 109–117.
Lau, S. Y. M., Taneja, A. K., & Hodges, R. S. (1984) *J. Biol. Chem. 259*, 13253–13261.
Macdonald, P. M., & Seelig, J. (1987) *Biochemistry 26*, 1231–1240.
Maduke, M., & Roise, D. (1993) *Science 260*, 364–367.
Marion, D., Zasloff, M., & Bax, A. (1988) *FEBS Lett. 227*, 21–26.
Matsuzaki, K., Handa, T., Miyajima, K., Mikura, Y., Shimizu, H., & Toguchi, H. (1988) *Chem. Pharm. Bull. 36*, 4253–4260.
Matsuzaki, K., Harada, M., Handa, T., Funakoshi, S., Fujii, N., Yajima, H., & Maiyajima, K. (1989a) *Biochim. Biophys. Acta 981*, 130–134.
Matsuzaki, K., Nakai, S., Handa, T., Takaishi, Y., Fujita, T., & Miyajima, K. (1989b) *Biochemistry 28*, 9392–9398.

Matsuzaki, K., Harada, M., Funakoshi, S., Fujii, N., & Miyajima, K. (1991a) *Biochim. Biophys. Acta 1063*, 162–170.
Matsuzaki, K., Takaishi, Y., Fujita, T., & Miyajima, K. (1991b) *Colloid Polym. Sci. 269*, 604–611.
Matsuzaki, K., Fukui, M., Fujii, N., & Miyajima, K. (1991c) *Biochim. Biophys. Acta 1070*, 259–264.
Matsuzaki, K., Fukui, M., Fujii, N., & Miyajima, K. (1993a) *Colloid Polym. Sci. 271*, 901–908.
Matsuzaki, K., Murase, O., Funakoshi, S., Fujii, N., & Miyajima, K. (1993b) in *Peptide Chemistry 1992; 2nd Japan Symposium on Peptide Chemistry* (Yanaihara, N., Ed.) pp 691–693, ESCOM Science Publishers, Leiden, The Netherlands.
Matsuzaki, K., Nakayama, M., Fukui, M.; Otaka, A., Funakoshi, S., Fujii, N., Bessho, K., & Miyajima, K. (1993c) *Biochemistry 32*, 11704–11710.
McKnight, C. J., Rafalski, M., & Gierasch, L. M. (1991) *Biochemistry 30*, 6241–6246.
Parente, R. A., Nir, S., & Szoka, F. C., Jr. (1990) *Biochemistry 29*, 8720–8728.
Rizzo, V., Stankowski, S., & Schwarz, G. (1987) *Biochemistry 26*, 2751–2759.
Schwarz, G. (1989) *Biochimie 71*, 1–9.
Schwarz, G., & Beschiaschvili, G. (1989) *Biochim. Biophys. Acta 979*, 82–90.
Schwarz, G., & Robert, C. H. (1992) *Biophys. Chem. 42*, 291–296.
Schwarz, G., Gerke, H., Rizzo, V., & Stankowski, S. (1987) *Biophys. J. 52*, 685–692.
Schwarz, G., Zong, R.-T., & Popescu, T. (1992) *Biochim. Biophys. Acta 1110*, 97–104.
Stankowski, S. (1983) *Biochim. Biophys. Acta 735*, 341–351.
Steiner, H., Andreu, D., & Merrifield, R. B. (1988) *Biochim. Biophys. Acta 939*, 260–266.
Takakuwa, T., Konno, T., & Meguro, H. (1985) *Anal. Sci. 1*, 215–218.
Thron, C. D. (1964) *J. Pharmacol. Exp. Ther. 145*, 194–201.
Voges, K.-P., Jung, G., & Sawyer, W. H. (1987) *Biochim. Biophys. Acta 896*, 64–76.
Weinstein, J. N., Klausner, R. D., Innerarity, T., Ralston, E., & Blumenthal, R. (1981) *Biochim. Biophys. Acta 647*, 270–284.
Weinstein, J. N., Ralson, E., Leserman, L. D., Klausner, R. D., Dragsten, P., Henkart, P., & Blumenthal, R. (1984) in *Liposome Technology* (Gregoriadis, G., Ed.) Vol. 3, pp 193–195, CRC Press, Boca Raton, FL.
Westerhoff, H. V., Hendler, R. W., Zasloff, M., & Juretić, D. (1989a) *Biochim. Biophys. Acta 975*, 361–369.
Westerhoff, H. V., Juretić, D., Hendler, R. W., & Zasloff, M. (1989b) *Proc. Natl. Acad. Sci. U.S.A. 86*, 6597–6601.
Williams, R. W., Starman, R., Taylor, K. M. P., Gable, K., Beeler, T., Zasloff, M., & Covell, D. (1990) *Biochemistry 29*, 4490–4496.
Winiski, A. P., McLaughlin, A. C., McDaniel, R. V., Eisenberg, M., & McLaughlin, S. (1986) *Biochemistry 25*, 8206–8214.
Zasloff, M. (1987) *Proc. Natl. Acad. Sci. U.S.A. 84*, 5449–5453.
Zasloff, M., Martin, B., & Chen, H.-C. (1988) *Proc. Natl. Acad. Sci. U.S.A. 85*, 910–913.